



High Order Coherence Functions and Spectral Distributions as Given by the Scully-Lamb Quantum Theory of the Laser

Tao Peng¹, Xingchen Zhao¹, Yanhua Shih² and Marlan O. Scully^{1,3,4*}

¹ Texas A&M University, College Station, TX, United States, ² University of Maryland, Baltimore County, Baltimore, MD, United States, ³ Baylor University, Waco, TX, United States, ⁴ Princeton University, Princeton, NJ, United States

We propose and demonstrate a method for measuring the time evolution of the off-diagonal elements $\rho_{n,n+k}(t)$ of the reduced density matrix obtained from the quantum theory of the laser. The decay rates of the off-diagonal matrix element $\rho_{n,n+k}(t)$ ($k = 2,3$) are measured for the first time and compared with that of $\rho_{n,n+1}(t)$, which corresponds to the linewidth of the laser. The experimental results agree with the Scully-Lamb quantum theory of the laser.

OPEN ACCESS

Edited by:

Tamar Seideman,
Northwestern University, United States

Reviewed by:

Qing Ai,

Beijing Normal University, China
Andre Bandrauk,
Université de Sherbrooke, Canada

*Correspondence:

Marlan O. Scully
scully@tamu.edu

Specialty section:

This article was submitted to
Optics and Photonics,
a section of the journal
Frontiers in Physics

Received: 22 January 2021

Accepted: 23 March 2021

Published: 21 April 2021

Citation:

Peng T, Zhao X, Shih Y and Scully MO
(2021) High Order Coherence
Functions and Spectral Distributions
as Given by the Scully-Lamb Quantum
Theory of the Laser.
Front. Phys. 9:657333.
doi: 10.3389/fphy.2021.657333

Keywords: high order coherence, quantum theory of the laser, spectral line distribution, density matrix, heterodyne detection

1. INTRODUCTION

Quantum coherence effects in molecular physics are largely based on the existence of the laser [1]. Indeed, in most of our experiments and calculations we take the laser to be an ideal monochromatic light source. If the laser linewidth is important then we usually just include a “phase diffusion” linewidth into the logic. But what if we are thinking about higher order correlation effects in an ensemble of coherently driven molecules. For example, photon correlation and light beating spectroscopy involving Glauber second order correlation functions [2, 3]. Furthermore, third and higher order photon correlations of the laser used to drive our molecular system can be important. The investigation of higher order quantum laser noise is the focus of the present paper.

Fifty years ago the Scully-Lamb (SL) quantum theory of the laser (QTL) was developed using a density matrix formalism [4]. In the interesting threshold region [5, 6] the steady state laser photon statistics is given by the diagonal elements of the laser density matrix as

$$\rho_{n,n} = \mathfrak{N} \prod_{m=0}^n [\alpha - \beta m]/\gamma, \quad (1)$$

where α is the linear gain, β is the non-linear saturation coefficient, γ is the cavity loss rate, and \mathfrak{N} is the normalization constant:

$$\mathfrak{N}^{-1} = \sum_n \prod_{m=0}^n [\alpha - \beta m]/\gamma. \quad (2)$$

Equation (1) is plotted in Figure 1 where it is compared with a coherent state.

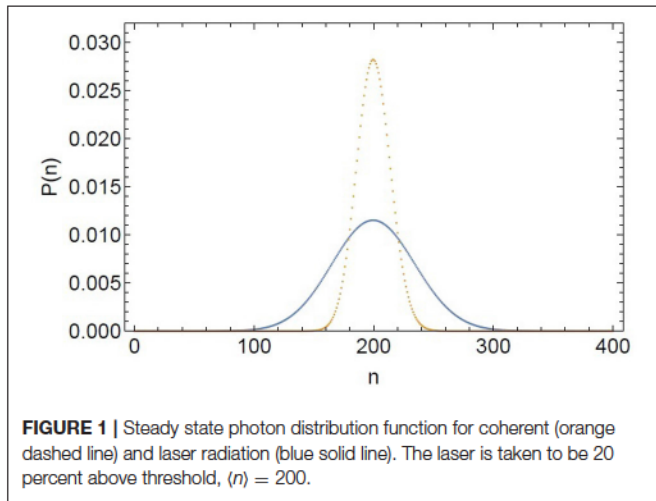


FIGURE 1 | Steady state photon distribution function for coherent (orange dashed line) and laser radiation (blue solid line). The laser is taken to be 20 percent above threshold, $\langle n \rangle = 200$.

TABLE 1 | Parameters in laser and BEC systems.

| Laser | BEC |
|----------|--------------------------------------------------------------------------------------------------------------------|
| α | Linear stimulated emission gain |
| β | Rate of cooling due to interaction with walls times the number of atom N |
| γ | Non-linear saturation due to the reabsorption of photons generated by stimulated emission |
| γ | Non-linearity parameter due to the constraint that there are N atoms in the BEC: numerically equal to α/N . |
| γ | Loss rate due to photons absorbed in cavity mirrors etc. |
| γ | Loss rate due to photon absorption from the thermal bath (walls) equal to $\alpha(T/T_c)^3$. |

The formalism developed in the QTL density matrix analysis has since been successfully applied to many other physical systems such as the single-atom maser(aka the micromaser) [7], the Bose-Einstein condensate (aka the atom laser, see Table 1) [8], pion physics [9], etc. Other applications of the formalism have been developed recently and more will likely emerge. Thus, we are motivated to deeper our understanding of the QTL by further analyzing and experimentally verifying the time dependence of off-diagonal elements $\rho_{n,n+k}(t) \equiv \rho_n^{(k)}(t)$. The diagonal elements of the laser density matrix for which $k = 0$, have been well-studied. Not as for the off-diagonal elements. In particular $\rho_n^{(1)}(t)$ yields the Schawlow-Townes laser linewidth. But what about the higher order correlations $k = 2, 3 \dots$? That is the focus of the current paper.

2. THEORY AND EXPERIMENT

The off-diagonal elements vanish at steady state, regressing to zero as [4]

$$\rho_n^{(k)}(t) = \rho_n^{(k)}(0) \exp(-k^2 D t) \quad (3)$$

where $D = \gamma/\bar{n}$ is the Schawlow-Townes phase diffusion linewidth and $\bar{n} = (\alpha - \gamma)/\beta$. The expectation value of the laser

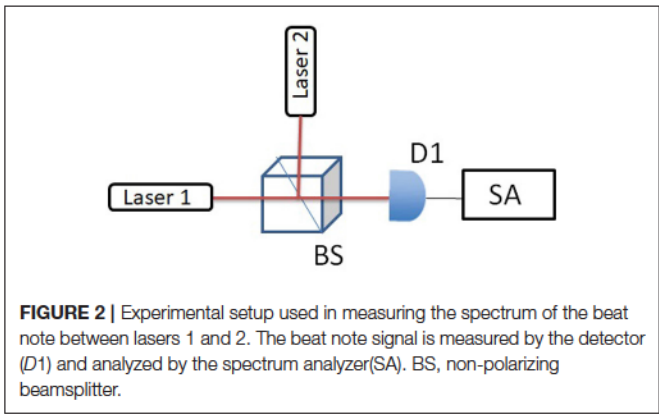


FIGURE 2 | Experimental setup used in measuring the spectrum of the beat note between lasers 1 and 2. The beat note signal is measured by the detector (D1) and analyzed by the spectrum analyzer(SA). BS, non-polarizing beam splitter.

amplitude operator is given by

$$\langle \hat{E}(z, t) \rangle = \mathcal{E}_0 e^{i\kappa z} \sum_n \rho_n^{(1)}(0) \sqrt{n+1} e^{-Dt} e^{-i\omega t}, \quad (4)$$

where ω is the center frequency of the laser field and the electric field per photon is given by $\mathcal{E}_0 = \sqrt{\hbar\omega/\epsilon_0 V}$, where ϵ_0 is the permittivity of free space and V is the laser cavity volume.

As is discussed in the following, the second order off-diagonal elements are given by the field operator averages

$$\langle \hat{E}(z, t) \hat{E}(z, t) \rangle = \mathcal{E}_0^2 e^{i2\kappa z} \sum_n \rho_n^{(2)}(0) \sqrt{(n+1)(n+2)} e^{-4Dt} e^{-i2\omega t}, \quad (5)$$

and the third order off-diagonal elements are given by

$$\begin{aligned} & \langle \hat{E}(z, t) \hat{E}(z, t) \hat{E}(z, t) \rangle \\ &= \mathcal{E}_0^3 e^{i3\kappa z} \sum_n \rho_n^{(3)}(0) \sqrt{(n+1)(n+2)(n+3)} e^{-9Dt} e^{-i3\omega t}. \end{aligned} \quad (6)$$

Equation (4) gives the time evolution associated with the first order off-diagonal elements $\rho_n^{(1)}$, yielding the spectral profile of the laser. The heterodyne method is usually adapted to measure the linewidth of the laser [10, 11], in which case the center frequency is shifted from optical frequency to the radio frequency range. A natural way to measure the laser linewidth is to beat two almost identical but uncorrelated lasers [12] such that the beat frequency between the lasers is in the MHz range. The result, as seen from Equation (10), is twice of the laser linewidth when the two independent lasers are nearly identical.

Many experiments have been carried out to determine the linewidth [10] and photon statistics [13] of the laser. Other experiments have measured the intensity correlation of the laser at threshold [14], revealing the influence of the intensity fluctuation on the laser spectrum. However, to the best of our knowledge, no measurements have been made of the higher order phase correlations ($k \geq 2$). Here we measure the second and third correlation of the heterodyne signals from two independent lasers, which yields the second and third order time evolution of a laser above threshold. Specifically, we performed the following

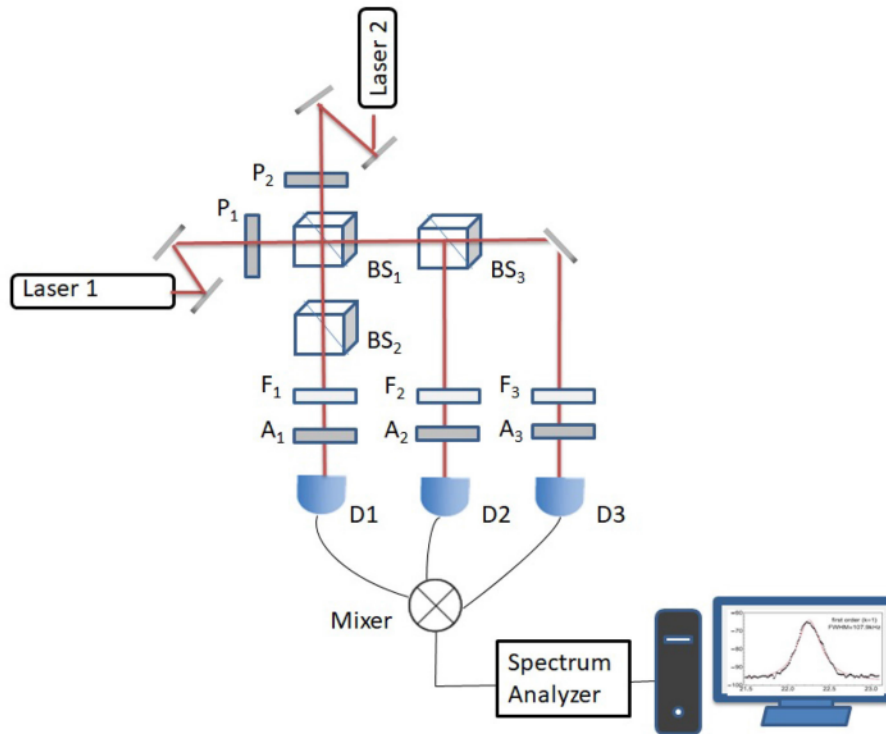


FIGURE 3 | Schematic setup for measuring higher order spectral line distribution up to 3rd order. Laser 1 and 2 : He-Ne lasers; P, polarizer; F, filter; A, analyzer; BS, non-polarizing beamsplitter; Mixer, frequency mixer; D1, D2, and D3, photodiode detectors.

experiments: the first set of experiments is to measure the spectral profile of the laser beat note, i.e., allows us to measure the decay rate as shown in Equation (4). The other two sets of experiments determine the spectral profile of the second and third order correlated beat notes, this allows us to measure the decay rate as shown in Equations (5) and (6).

Figure 2 illustrates the setup of the first set of experiments. This is a typical heterodyne detection setup, the center frequency between the two He-Ne lasers is in the MHz range. This difference allows us to analyze the beat signal around a non-zero value hence the full shape of the linewidth is obtained unambiguously. A non-polarizing beamsplitter (BS) is used to mix the two laser beams. The beat signal is then directed to the photodiode (D1) after the BS. A fast Fourier transform (FFT) of the signal is performed by the spectrum analyzer (SA) giving the frequency spectrum of the beat note.

For the first set of experiments, the first order coherence function [3, 4] is

$$\begin{aligned}
 G^{(1)}(t) &= \text{Tr}\{\rho[(\hat{E}_1^\dagger(t) + \hat{E}_2^\dagger(t))(\hat{E}_1(t) + \hat{E}_2(t))]\} \\
 &= \text{Tr}((\rho_1 \otimes \rho_2)[|\hat{E}_1(t)|^2 + |\hat{E}_2(t)|^2 + \hat{E}_1^\dagger(t)\hat{E}_2(t) + c.c.]) \\
 &= \mathcal{E}_1^2 \text{Tr}[\rho_1 \hat{a}_1^\dagger(t) \hat{a}_1(t)] + \mathcal{E}_2^2 \text{Tr}[\rho_2 \hat{a}_2^\dagger(t) \hat{a}_2(t)] \\
 &+ \mathcal{E}_1 \mathcal{E}_2 \{\text{Tr}[(\rho_1 \otimes \rho_2) \hat{a}_1^\dagger(t) \hat{a}_2(t)] e^{i(v_2 - v_1)t} + c.c.\}, \quad (7)
 \end{aligned}$$

where $\rho = \rho_1 \otimes \rho_2$ is the density operator of the system, ρ_1 and ρ_2 represent the density operators of laser 1 and 2, v_1 and v_2 represent the center frequencies of the lasers 1 and 2, respectively.

From the above equation, we can see the only terms that carry the beat note frequency are

$$\Gamma^{(1)}(t) = \mathcal{E}_1 \mathcal{E}_2 \text{Tr}[(\rho_1 \otimes \rho_2) \hat{a}_1^\dagger(t) \hat{a}_2(t)] e^{i(v_2 - v_1)t}, \quad (8)$$

with its complex conjugate which contributes to the $-v_0$ frequency component, where $v_0 \equiv v_2 - v_1$. Under the condition that the two lasers are independent, we can rewrite Equation (8) as

$$\begin{aligned}
 \Gamma^{(1)}(v_0, t) &= \mathcal{E}_1 \sum_{n_1} \sqrt{n_1 + 1} \rho_{n_1}^{(1)}(0) e^{-D_1 t} e^{-i v_1 t} \\
 &\times \mathcal{E}_2 \sum_{n_2} \sqrt{n_2} \rho_{n_2}^{(-1)}(0) e^{-D_2 t} e^{i v_2 t}. \quad (9)
 \end{aligned}$$

Taking the Fourier transform, we have a Lorentzian spectrum centered at the beat frequency v_0 with a width $D' = D_1 + D_2$, which is essentially twice the width of one laser

$$S_{v_0}(\omega) \propto \frac{D'}{(\omega - v_0)^2 + (D')^2}. \quad (10)$$

The second and third experiments measure the spectral profile of the second and third order correlation of beat notes, the setup is

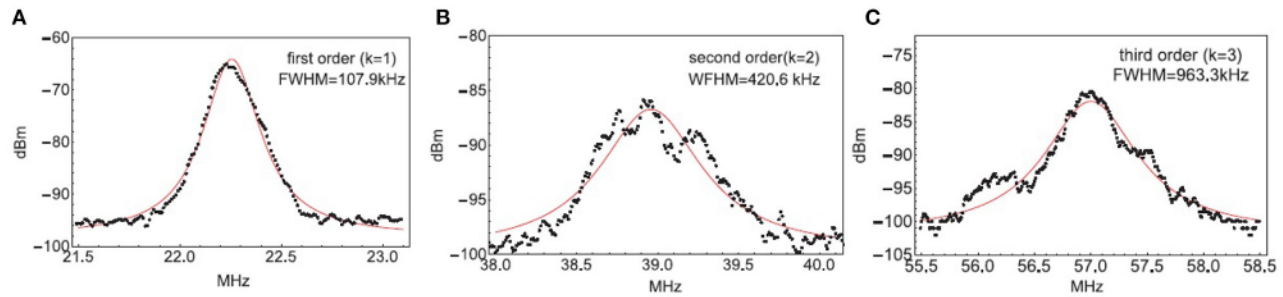


FIGURE 4 | Experimental results from the two sets of measurements. The bandwidths of the detectors are 50 MHz, the resolution bandwidth of the SA is 10 kHz. The black dots are experimental data and the red curves are theory. **(A)** is the beat signals from D_1 , where the FWHM is 107.9 kHz with average 50 times. Theory is the Fourier transform of the laser fields time evolution ($e^{-D't}$) associated with frequency ν_0 , as shown in Equation (10); **(B)** is correlated signal from D_1 and D_2 , where the FWHM bandwidth is 420.6 kHz with average 50 times. Theory is the Fourier transform of the correlated laser fields time evolution ($e^{-4D't}$) associated with frequency $2\nu_0$, as shown in Equation (13). **(C)** is correlated signal from D_1 , D_2 , and D_3 , where the FWHM is 963.3 kHz with average 50 times. Theory is the Fourier transform of the correlated laser fields time evolution ($e^{-9D't}$) associated with frequency $3\nu_0$, as shown in Equation (16).

shown in Figure 3. We used the same two lasers to create the beat signal, where three detectors $D_i (i = 1, 2, 3)$ are used. The outputs from the photodiodes are used as inputs for a frequency mixer. The output from the mixer is then sent to the spectrum analyzer and the frequency spectrum of the correlated signal is obtained after the FFT. As shown in Figure 3, this set of experiments measures the laser field correlation that is governed by the time evolution of the second and third order off-diagonal elements $\rho_n^{(2)}(t)$ and $\rho_n^{(3)}(t)$, respectively. The quantity we now measure is determined by the correlation of the heterodyne signals from detectors as in Figure 3. We have the signal of interest at frequency $2\nu_0$ from the second order coherence function is

$$\Gamma^{(2)}(t) = \mathcal{E}_1^2 \mathcal{E}_2^2 \text{Tr}(\rho_1 \otimes \rho_2) \hat{a}_1^\dagger(t) \hat{a}_1^\dagger(t) \hat{a}_2(t) \hat{a}_2(t) e^{i2\nu_0 t}. \quad (11)$$

The correlated heterodyne signal is

$$\begin{aligned} \Gamma^{(2)}(2\nu_0, t) &= \mathcal{E}_1^2 \sum_{n_1} \rho_{n_1}^{(2)}(0) \sqrt{(n_1 + 2)(n_1 + 1)} e^{-4D_1 t} e^{-i2\nu_1 t} \\ &\times \mathcal{E}_2^2 \sum_{n_2} \rho_{n_2}^{(-2)}(0) \sqrt{(n_2 - 1)n_2} e^{-4D_2 t} e^{i2\nu_2 t}. \end{aligned} \quad (12)$$

Taking the Fourier transform, we get a Lorentzian spectral profile centered at $2\nu_0$ with a width of $4D'$

$$S_{2\nu_0}(\omega) \propto \frac{4D'}{(\omega - 2\nu_0)^2 + (4D')^2}. \quad (13)$$

similarly, the signal of interest at frequency $3\nu_0$ from the third order coherence function is

$$\Gamma^{(3)}(t) = \mathcal{E}_1^3 \mathcal{E}_2^3 \text{Tr}(\rho_1 \otimes \rho_2) \hat{a}_1^\dagger(t) \hat{a}_1^\dagger(t) \hat{a}_1^\dagger(t) \hat{a}_2(t) \hat{a}_2(t) \hat{a}_2(t) e^{i3\nu_0 t}. \quad (14)$$

The correlated heterodyne signal is

$$\begin{aligned} \Gamma^{(3)}(3\nu_0, t) &= \mathcal{E}_1^3 \sum_{n_1} \rho_{n_1}^{(3)}(0) \sqrt{(n_1 + 3)(n_1 + 2)(n_1 + 1)} e^{-9D_1 t} e^{-i3\nu_1 t} \\ &\times \mathcal{E}_2^3 \sum_{n_2} \rho_{n_2}^{(-3)}(0) \sqrt{(n_2 - 2)(n_2 - 1)n_2} e^{-9D_2 t} e^{i3\nu_2 t}. \end{aligned} \quad (15)$$

We therefore get a Lorentzian spectral profile centered at $3\nu_0$ with a width of $9D'$

$$S_{3\nu_0}(\omega) \propto \frac{9D'}{(\omega - 3\nu_0)^2 + (9D')^2}. \quad (16)$$

The main experimental results are shown in Figure 4. All measurements were taken with the laser operating at the same average output power level. The resolution bandwidth (RBW) of the SA is 10 kHz, video bandwidth (VBW) is 30 kHz in all the measurements. For the sake of simplicity, the Full width at half maximum (FWHM) linewidth is taken at the -3 dB width of the measured spectrum by considering only the Lorentzian fitting [12]. Figure 4A represents the data of the first set of experiments with an average of 50 measurements of beat note signal from D_1 . The theoretical fitting in the red solid line is based on Equation (10), and the FWHM is 107.9 kHz. Figure 4B represents the data of the second set of experiments with 50 measurements of correlated beat note signals from D_1 and D_2 . The theoretical fitting in the red solid line is based on Equation (13), and the FWHM is estimated to be 420.6 kHz. Figure 4C represents the data of the third order experiments with 50 measurements from all three detectors. The theoretical fitting in the red solid line is based on Equation (16), and the FWHM is estimated to be 963.3 kHz. First of all, we see that the obtained linewidth from the second order correlation spectrum is essentially 4 times wider than that of the single beat note linewidth, as well as the third order spectrum is 9 times wider than that of the single beat note linewidth, validating our theoretical expectation. Secondly, we see that the theoretical

curves fit the data well in the center peak, but not as good at the tails. This is mainly due to the influences from other noises that also contribute to the spectral profile. For the same reason, we see that the single beat note signal can be better fitted than the second and third order correlation signals. There are some small peaks in the higher order measurements, due to our remeasured higher order spectral signal is close to the noise level of the detection system. Ideally, more averaging ($\gg 50$) should be able to smooth out these peaks. However, we note here that, there is a trade-off between time averaging and the accurate measurement of the center beat note frequency, due to the drifting of center frequencies of the two lasers. Further using an intense local oscillator and sensitive detection system (detector and spectral analyzer) should be able to solve this issue. Nevertheless, our data confirms the Lorentizan spectral profile of the signal and the time evolution described by Equation (3), in the case of $k = 1$, $k = 2$, and $k = 3$.

3. CONCLUSION

In conclusion, we have studied the time evolution of the higher degrees of off-diagonality obtained SL theory of the laser. We particularly measured the bandwidth of the laser beat note and the bandwidth of the correlated laser beat note, which reveal the evolution of the first, second, and third order off-diagonal elements of the laser density operator. The higher order spectra reveal the influence of the randomness in the phase of the laser field due to quantum fluctuation. Experimental results agreed with the SL QTL showing that the bandwidth

of the third order and second order spectral profile are nine times and four times wider than that of the first order spectral profile, respectively.

DATA AVAILABILITY STATEMENT

The raw data supporting the conclusions of this article will be made available by the authors, without undue reservation.

AUTHOR CONTRIBUTIONS

TP, YS, and MS discussed the design principle. TP and XZ performed the experiment and data analysis. TP and MS wrote the paper. All the authors polished the paper.

FUNDING

This study was funded by Air Force Office of Scientific Research (Award No. FA9550-20-1-0366 DEF), Office of Naval Research (Award No. N00014-20-1-2184), Robert A. Welch Foundation (Grant No. A-1261), National Science Foundation (Grant No. PHY-2013771), King Abdulaziz City for Science and Technology (KACST).

ACKNOWLEDGMENTS

We thank Z. H. Yi, R. Nessler, H. Cai, and J. Sprigg for helpful discussion.

REFERENCES

1. Pestov D, Murawski RK, Ariunbold GO, Wang X, Zhi M, Sokolov AV, et al. Optimizing the laser-pulse configuration for coherent Raman spectroscopy. *Science*. (2007) 316:265–8. doi: 10.1126/science.1139055
2. Cummins H. *Photon Correlation and Light Beating Spectroscopy*. Vol. 3. Springer Science & Business Media (2013).
3. Glauber RJ. The quantum theory of optical coherence. *Phys Rev*. (1963) 130:2529. doi: 10.1103/PhysRev.130.2529
4. Scully M, Lamb W Jr. Quantum theory of an optical maser. *Phys Rev Lett*. (1966) 16:853.
5. Haken H. Theory of intensity and phase fluctuations of a homogeneously broadened laser. *Z Phys*. (1966) 190:327–56. doi: 10.1007/BF01333598
6. DeGiorgio V, Scully MO. Analogy between the laser threshold region and a second-order phase transition. *Phys Rev A*. (1970) 2:1170. doi: 10.1103/PhysRevA.2.1170
7. Meschede D, Walther H, Müller G. One-atom maser. *Phys Rev Lett*. (1985) 54:551. doi: 10.1103/PhysRevLett.54.551
8. Scully MO. Condensation of N bosons and the laser phase transition analogy. *Phys Rev Lett*. (1999) 82:3927. doi: 10.1103/PhysRevLett.82.3927
9. Hoang T. Remarks on the charged multiplicity of hadronic Z 0 (91) decays. *Z Phys C Part Fields*. (1997) 73:149–52. doi: 10.1007/s002880050304
10. Okoshi T, Kikuchi K, Nakayama A. Novel method for high resolution measurement of laser output spectrum. *Electron Lett*. (1980) 16:630–1. doi: 10.1049/el:19800437
11. Richter L, Mandelberg H, Kruger M, McGrath P. Linewidth determination from self-heterodyne measurements with subcoherence delay times. *IEEE J Quant Electron*. (1986) 22:2070–4. doi: 10.1109/JQE.1986.1072909
12. Muanzaula L, Ravi H, Sylvan K, Natarajan V. Measuring the linewidth of a stabilized diode laser. *arXiv preprint arXiv:151003683* (2015).
13. Arecchi FT. Measurement of the statistical distribution of Gaussian and laser sources. *Phys Rev Lett*. (1965) 15:912. doi: 10.1103/PhysRevLett.15.912
14. Corti M, Degiorgio V, Arecchi F. Measurements of the fine structure of laser intensity correlations near threshold. *Opt Commun*. (1973) 8:329–32. doi: 10.1016/0030-4018(73)90207-1

Conflict of Interest: The authors declare that the research was conducted in the absence of any commercial or financial relationships that could be construed as a potential conflict of interest.

Copyright © 2021 Peng, Zhao, Shih and Scully. This is an open-access article distributed under the terms of the Creative Commons Attribution License (CC BY). The use, distribution or reproduction in other forums is permitted, provided the original author(s) and the copyright owner(s) are credited and that the original publication in this journal is cited, in accordance with accepted academic practice. No use, distribution or reproduction is permitted which does not comply with these terms.